Optimal active random vibration control for smart truss structures based on reliability

W Gao[1,2*] and **N Zhang**[2]
[1]School of Mechanical and Manufacturing Engineering, The University of New South Wales, Sydney, Australia
[2]Mechatronics and Intelligent Systems, University of Technology, Sydney, Australia

The manuscript was received on 13 April 2006 and was accepted after revision for publication on 18 July 2007.

DOI: 10.1243/09544062JMES365

Abstract: The current paper presents the reliability-based optimization of the location and feedback gains of active bar in a closed-loop control system for random smart truss structures under stationary random excitation. The mathematical model with reliability constraints on the root mean square value of the structural random dynamic displacement and stress response is developed based on maximization of dissipation energy due to the control action. The randomness of the structural physical materials, geometry, and damping are included in the analysis, and the applied forces are considered as stationary random excitation. The numerical characteristic corresponding to mean values and standard deviations of the stationary random responses of random smart structures is developed by the random factor method. Numerical examples of truss structures are presented to demonstrate the rationality and validity of the active control model.

Keywords: random smart truss structures, reliability constraints, random vibration, optimization

1 INTRODUCTION

The field of smart or intelligent structures has raised much interest over the past decade [**1–3**]. Unlike the conventional engineering structures which are passive, smart structures has the ability to perform self-diagnosis and adapt to the environment change. A piezoelectric (PZT) smart truss structure is used in spacecraft deployable antenna, large antennas, and other important large-scale truss structures, in which the PZT active bar can be used as both an actuator for vibration excitation, and sensor for vibration measurement. Optimal placement of the PZT active bar is an important factor in the process of the structural design phase, and its shape and vibration control. The location of active bars in the smart truss structure directly affects the validity of active vibration control.

Recently, there has been much work published on the optimization of smart structures. Wang and Wang [**4**] proposed a controllability index to quantify the controllability factor based on the state-coupled equation of beam structures with PZT actuators and the index was utilized as an objective function to determine the optimal locations of PZT actuators for vibration control of beam structures. Suk *et al.* [**5**] introduced the Lyapunov control law for the slew manoeuvre of a flexible space structure by using a time-domain finite-element analysis. To optimize the gain set of the control system, an energy-based performance index was adopted, and the gradients of the performance index with respect to each gain were derived. Quek *et al.* [**6**] proposed a simple optimal placement strategy of PZT sensor/actuator pairs for vibration control of laminated composite plate, where the active damping effect under a classical control framework is maximized using the finite-element approach. Chen and Lin [**7**] proposed a systematic method based on the impedance technique to determine the optimal locations and shapes of multiple-induced strain actuators bonded on a host structure in respect of the smallest power consumption. Peng *et al.* [**8**] proposed a performance criterion for the optimization of PZT patch actuator locations

Corresponding author: Mechatronics and Intelligent Systems, Faculty of Engineering, University of Technology, Sydney, NSW 2007, Australia. email: wei.gao@uts.edu.au or wgao@eng.uts.edu.au

on flexible plate structures based on maximizing the controllability grammian, and the genetic algorithm was used to implement the optimization.

To date, the majority of modelling on optimization of active vibration control using PZT smart structures has used deterministic models (DMs) to model the dynamic response of smart structures, and optimal placement of the PZT actuators and sensors. In these cases, the structural parameters, applied loads and control forces are regarded as known parameters. However, DMs of the dynamic response associated with smart structures cannot reflect the influence of the randomness of the structural parameters. The dynamic response of an engineering structure can be sensitive to randomness in its parameters arising from variability in its geometric or material parameters, or randomness resulting from the assembly process and manufacturing tolerances. In addition, applied loads can be random process forces, such as wind, earthquakes, and blast shock. The problem of stochastic smart structures subject to random applied excitation is of great significance in realistic engineering applications.

The dynamic characteristics and dynamic response analysis of a closed-loop control system for an intelligent structure is an important segment in the process of its design and vibration control. For the dynamic analysis of structures with uncertainties, the Monte-Carlo method (MCM), perturbation method (PM), and stochastic finite-element method (SFEM) are widely used. In the MCM, the values of the structural parameters are changed within a given range. A large amount of dynamic analyses on the same structure is then performed, and the statistical data (mean value and standard deviation) of the natural frequencies, mode shapes, and dynamic response are obtained [**9**, **10**]. In practice, this is the method of last resort since the attendant computational cost can be prohibitive for systems modelled using a large number of degrees of freedom. The PM uses a combination of matrix perturbation theory, finite-element method and Taylor series expansion to obtain the dynamic characteristics of stochastic structures [**11**]. The major drawback of such local approximation techniques is that the results become highly inaccurate when the coefficients of variation of the input random variables are increased [**12**]. In the SFEM, uncertainties are represented by random variables or random fields. To enable a computational treatment of this problem, the random fields are first discretized to represent them in terms of a finite number of random variables. Subsequent application of spatial and temporal discretization schemes leads to a system of random algebraic equations to be solved for the response process. In order for the SFEM to be practical for large-scale systems, it is essential that efficient numerical schemes be available for solving random algebraic equations arising from discretization of stochastic partial differential equations in space, time, and the random dimension of the problem. In 1990, Ghanem and Spanos [**13**] proposed the spectral SFEM for the solution of problems of structural mechanics involving material variability which was modelled as a stochastic process. The Karhunen–Loeve expansion is used to represent this process in a computationally expedient manner by means of a set of random variables and the well-established deterministic finite-element method is used to discretize the differential equations governing the structural response. The new method allows the computation of the probability distribution functions of the response variables in an expeditious manner. Elishakoff *et al.* [**14**] proposed an alternative way of constructing the global stiffness matrix of the finite-element method for bending beams, it also applies the new formulation to first and second moment analysis of stochastic beams, which involve spatially uncertain bending stiffness. Graham and Deodatis [**15**] studied the variability of the random response displacements and eigenvalues of structures with multiple uncertain material and geometric properties by using variability response functions. The material and geometric properties are assumed to be described by cross-correlated stochastic fields. The variance of the displacement/eigenvalue is expressed as the sum of integrals that involve the auto-spectral density functions characterizing the structural properties, the cross-spectral density functions between the structural properties, and the deterministic variability response functions. Recently, the dynamic response of stochastic structures under random excitation has received research attention. Zhao and Chen [**16**] studied vibration of structures with random parameters to random excitation using Neumann SFEM. Li and Liao [**17**] investigated the use of the orthogonal expansion method with the pseudo-excitation method for analysing the dynamic response of structures with uncertain parameters under external random excitation. Ma *et al.* [**18**] solved the evolutionary earthquake response problem of an uncertain structure with bounded random parameters by a unified approach. Li and Chen [**19**] proposed a new method based on probability density evolution method to construct the probability density evolution equation and obtain the numerical characteristics of random structural dynamic response.

In the current paper, optimization of the location of the active bar and feedback gain in PZT random smart truss structures are investigated. The randomness of the structural materials, geometry, and damping are simultaneously considered. The applied force is taken as a stationary random excitation. Numerical expressions for the mean values and standard deviations of the natural frequencies and modeshapes, and displacement and stress responses of smart truss structures are obtained. The performance function due to the control action is based on maximization of the dissipation energy. To formulate the optimal control problem, the algorithm for a linear quadratic regulator with output feedback has been employed in this paper. An optimal mathematical model with reliability constraints on the root mean square value of structural dynamic displacement and stress response is developed. Numerical examples of stochastic smart truss structures are presented to demonstrate the rationality and validity of the active control model.

2 MATHEMATICAL MODEL OF THE OPTIMIZATION PROBLEM

Following the finite-element formulation, the equation of motion for an intelligent structure is given by

$$[\mathbf{M}]\{\ddot{\boldsymbol{u}}(t)\} + [\mathbf{C}]\{\dot{\boldsymbol{u}}(t)\} + [\mathbf{K}]\{\boldsymbol{u}(t)\} = \{\boldsymbol{F}(t)\} + [\mathbf{B}]\{\boldsymbol{F}_{\mathrm{C}}(t)\} \tag{1}$$

In the following analysis, the Wilson's damping hypothesis [20] is adopted. Using the modal expansion $\{\boldsymbol{u}(t)\} = [\boldsymbol{\phi}]\{z(t)\}$, the equation of motion takes the form

$$[\mathbf{I}]\{\ddot{z}(t)\} + [\mathbf{D}]\{\dot{z}(t)\} + [\boldsymbol{\Omega}]\{z(t)\} = [\boldsymbol{\phi}]^{\mathrm{T}}\{\boldsymbol{F}(t)\} + [\boldsymbol{\phi}]^{\mathrm{T}}[\mathbf{B}]\{\boldsymbol{F}_{\mathrm{C}}(t)\} \tag{2}$$

where $[\mathbf{D}] = \mathbf{diag}[2\zeta_j\omega_j]$, $[\boldsymbol{\Omega}] = \mathbf{diag}[\omega_j^2]$ for $j = 1, \ldots, n$.

For active control of the truss bar, a velocity feedback control law is considered. Since each active bar can be considered as a collocated actuator/sensor pair, the output matrix is the transpose of the input matrix. The output vector $\boldsymbol{Y}(t)$ and control force vector $\{\boldsymbol{F}_{\mathrm{C}}(t)\}$ can be, respectively, expressed as

$$\boldsymbol{Y}(t) = [\mathbf{B}]^{\mathrm{T}}[\boldsymbol{\phi}]\{\dot{z}(t)\} \tag{3}$$

$$\{\boldsymbol{F}_{\mathrm{C}}(t)\} = -[\mathbf{G}]\boldsymbol{Y}(t) = -[\mathbf{G}][\mathbf{B}]^{\mathrm{T}}[\boldsymbol{\phi}]\{\dot{z}(t)\} \tag{4}$$

where $[\mathbf{G}] = \mathbf{diag}\{g_j\}$ is the gain matrix [21]. Substituting equation (4) into equation (2) yields the equation of the closed-loop system

$$[\mathbf{I}]\{\ddot{z}(t)\} + ([\mathbf{D}] + [\boldsymbol{\phi}]^{\mathrm{T}}[\mathbf{B}][\mathbf{G}][\mathbf{B}]^{\mathrm{T}}[\boldsymbol{\phi}])\{\dot{z}(t)\} + [\boldsymbol{\Omega}]\{z(t)\} = [\boldsymbol{\phi}]^{\mathrm{T}}\{\boldsymbol{F}(t)\} \tag{5}$$

In the state-space representation, the equation of motion for the closed-loop system becomes

$$\{\dot{\boldsymbol{u}}(t)\} = [\mathbf{A}]\{\boldsymbol{u}(t)\} \tag{6}$$

where

$$\{\boldsymbol{u}\} = \{z(t)\dot{z}(t)\}^{\mathrm{T}} \tag{7}$$

$$[\mathbf{A}] = \begin{bmatrix} 0 & [\mathbf{I}] \\ -[\boldsymbol{\Omega}] & -([\mathbf{D}] + [\boldsymbol{\phi}]^{\mathrm{T}}[\mathbf{B}][\mathbf{G}][\mathbf{B}]^{\mathrm{T}}[\boldsymbol{\phi}]) \end{bmatrix} \tag{8}$$

Both the optimal location of the active bar, and the optimal gain of the closed-loop control system are determined such that the total energy dissipated in the system is maximized. The total energy dissipated in the system is taken as the performance and it can be expressed as

$$J = \int_0^\infty \{\dot{z}(t)\}^{\mathrm{T}}[\boldsymbol{\phi}]^{\mathrm{T}}\left([\mathbf{D}] + [\mathbf{B}][\mathbf{G}][\mathbf{B}]^{\mathrm{T}}\right)[\boldsymbol{\phi}]\{\dot{z}(t)\}\,\mathrm{d}t \tag{9}$$

The equation (9) can also be expressed as [22]

$$J = \{\boldsymbol{u}(0)\}^{\mathrm{T}} \int_0^\infty e^{[\mathbf{A}]^{\mathrm{T}}t}[\mathbf{Q}]e^{[\mathbf{A}]t}\mathrm{d}t\{\boldsymbol{u}(0)\} \tag{10}$$

where $[\mathbf{Q}] = \begin{bmatrix} [\boldsymbol{\Omega}] & 0 \\ 0 & [\mathbf{I}] \end{bmatrix}$. Making use of the method described in reference [22], the performance function can be expressed as

$$J = tr[\mathbf{W}] \tag{11}$$

where the matrix $[\mathbf{W}]$ can be obtained by solving the following equation

$$[\mathbf{A}]^{\mathrm{T}}[\mathbf{W}] + [\mathbf{W}][\mathbf{A}] = [\mathbf{Q}] \tag{12}$$

For the smart truss structure with random parameters, and where the load is a stationary random excitation, an optimization program is written with reliability constraints that implements the following steps. For a fixed gain ($g = g_j$), the optimal location of the active bar (that is, the optimal $[\mathbf{B}]$ matrix) is obtained such that the total energy dissipated J is maximized. After the optimal placement of the active bar is determined, the feedback gain is then optimized. This is achieved by calculating the mean square displacement for each kth degree of freedom and mean square dynamic stress for each eth element. Reliability constraints are placed on the root mean square displacement and stress, respectively, as follows

$$R^*_{\psi_\sigma} - P_r\left\{\psi^*_\sigma - \max(\psi_{\sigma e}) \geqslant 0\right\} \leqslant 0, \quad e = 1, 2, \ldots, m \tag{13}$$

$$R^*_{\psi_u} - P_r\left\{\psi^*_u - \max(\psi_{uk}) \geqslant 0\right\} \leqslant 0, \quad k = 1, 2, \ldots, n \tag{14}$$

$$[\mathbf{B}] \subset [\mathbf{B}^*], \quad [\mathbf{G}] < [\mathbf{G}^*] \tag{15}$$

$[\mathbf{B}]$ and $[\mathbf{G}]$ are the design variables. $P_r\{\cdot\}$ is the reliability obtained from the actual calculation. In this model, [**B**], [**G**], $R^*_{\psi_\sigma}$, $R^*_{\psi_u}$, $P_r\{\cdot\}$, ψ^*_σ, and ψ^*_u can be random variables or deterministic values. [$\mathbf{B}^*$] and [$\mathbf{G}^*$] are the upper bounds of [**B**] and [**G**], respectively.

In the above model, the dynamic stress and response constraints are expressed by the probability form, which makes the optimal problem difficult to solve. For this reason, the reliability constraints are transformed into normal constraints by means of the second-order moment theory on the reliability [**23**]. Hence, the reliability constraints equations (13) and (14) can be, respectively, expressed as

$$\beta^*_{\psi_\sigma} - \frac{\mu_{\psi^*_\sigma} - \mu_{\max(\psi_{\sigma e})}}{\left(\sigma^2_{\psi^*_\sigma} + \sigma^2_{\max(\psi_{\sigma e})}\right)^{1/2}} \leqslant 0, \quad e = 1, 2, \ldots, m \quad (16)$$

$$\beta^*_{\psi_u} - \frac{\mu_{\psi^*_u} - \mu_{\max(\psi_{uk})}}{\left(\sigma^2_{\psi^*_u} + \sigma^2_{\max(\psi_{uk})}\right)^{1/2}} \leqslant 0, \quad k = 1, 2, \ldots, n \quad (17)$$

where $\beta^*_{\psi_\sigma} = \Phi^{-1}(R^*_{\psi_\sigma})$ and $\beta^*_{\psi_u} = \Phi^{-1}(R^*_{\psi_u})$ are the given reliability of the maximum root mean square value of the dynamic stress response and displacement, respectively. $\mathbf{\Phi}^{-1}(\cdot)$ denotes the inverse function of the normal distribution of random variables.

3 SMART STRUCTURAL STATIONARY RANDOM RESPONSE

Suppose that there are m elements in the smart truss structure under consideration. In the structure, any element can be taken as either a passive or active bar, where a PZT bar is used as the active bar. In the stiffness and the mass matrices of the smart truss structures in global coordinates can be expressed as

$$[\mathbf{K}] = \sum_{e=1}^{m} [\mathbf{K}_e] = \sum_{e=1}^{m} \left\{ [\mathbf{T}_e]^{\mathrm{T}} \left[\theta \frac{E_e A_e}{l_e} + (1-\theta) \frac{c_{33e} + (e_{33e})^2/\varepsilon_{33e}}{l^{\mathrm{C}}_e} A^{\mathrm{C}}_e \right] [\bar{\mathbf{G}}][\mathbf{T}_e] \right\} \quad (18)$$

$$[\mathbf{M}] = \sum_{e=1}^{m} [\mathbf{M}_e] = \sum_{e=1}^{m} \left\{ \frac{1}{2} (\theta \rho_e A_e l_e + (1-\theta) \rho^{\mathrm{C}}_e A^{\mathrm{C}}_e l^{\mathrm{C}}_e) [\mathbf{I}] \right\} \quad (19)$$

where θ is a Boolean algebra value defined by the following: when $\theta = 0$, the mixed element is a PZT active element bar; when $\theta = 1$, the mixed element is a passive element bar. [**I**] is a sixth-order identity matrix. [$\bar{\mathbf{G}}$] is a 6×6 matrix, where $\bar{g}_{11} = \bar{g}_{44} = 1$, $\bar{g}_{14} = \bar{g}_{41} = -1$, and other elements are zero [**24**]. [$\mathbf{T}_e$] is the transformation matrix that translates the local coordinates of the eth element to global coordinates, and $[\mathbf{T}_e]^{\mathrm{T}}$ is its transpose. E^{C}_e is the generalized Young's modulus of the PZT active bar which considers the mechanic–electronic coupling effect, and is given by

$$E^{\mathrm{C}}_e = c_{33e} + \frac{(e_{33e})^2}{\varepsilon_{33e}} \quad (20)$$

Substituting the equation (20) into equation (18) yields

$$[\mathbf{K}] = \sum_{e=1}^{m} [\mathbf{K}_e] = \sum_{e=1}^{m} \left\{ \left[\theta \frac{E_e A_e}{l_e} + (1-\theta) \frac{E^{\mathrm{C}}_e A^{\mathrm{C}}_e}{l^{\mathrm{C}}_e} \right] [\mathbf{T}] \right\} \quad (21)$$

In the closed-loop control system, since the control force is determined by the applied force, the control force is a random force vector, and these two variables have full positive correlation. Let

$$\{\boldsymbol{P}(t)\} = \{\boldsymbol{F}(t)\} + [\mathbf{B}]\{\boldsymbol{F}_{\mathrm{C}}(t)\} \quad (22)$$

Equation (1) can be rewritten as

$$[\mathbf{M}]\{\ddot{\boldsymbol{u}}(t)\} + [\mathbf{C}]\{\dot{\boldsymbol{u}}(t)\} + [\mathbf{K}]\{\boldsymbol{u}(t)\} = \{\boldsymbol{P}(t)\} \quad (23)$$

Equation (23) is a set of coupled differential equations. Its formal solution can be obtained in terms of the decoupling transform and Duhamel integral [**18**], that is

$$\{\boldsymbol{u}(t)\} = \int_0^t [\boldsymbol{\phi}][\mathbf{h}(\tau)][\boldsymbol{\phi}]^{\mathrm{T}} \{\boldsymbol{P}(t-\tau)\}\, \mathrm{d}\tau \quad (24)$$

[$\mathbf{h}(t)$] is the impulse response function matrix of the structure, and can be expressed as

$$[\mathbf{h}(t)] = \mathbf{diag}\{h_j(t)\} \quad (25)$$

$$h_j(t) = \begin{cases} \dfrac{1}{\omega'_j} \exp(-\zeta_j \omega_j t) \times \sin \omega'_j t & t \geqslant 0 \\ 0 & t < 0 \end{cases}, \quad j = 1, 2, \ldots, n \quad (26)$$

where $\omega'_j = \omega_j (1 - \zeta^2_j)^{1/2}$. From equation (24), the correlation function matrix of the displacement response of the structure can be obtained

$$\begin{aligned} [\mathbf{R}_u(\varepsilon)] &= E\left(\{\boldsymbol{u}(t)\}\{\boldsymbol{u}(t+\varepsilon)\}^{\mathrm{T}}\right) \\ &= \int_0^t \int_0^t [\boldsymbol{\phi}][\mathbf{h}(\tau)][\boldsymbol{\phi}]^{\mathrm{T}} [\mathbf{R}_{\mathrm{P}}(\tau - \tau_1 + \varepsilon)][\boldsymbol{\phi}] \\ &\quad \times [\mathbf{h}(\tau_1)]^{\mathrm{T}} [\boldsymbol{\phi}]^{\mathrm{T}} \mathrm{d}\tau\, \mathrm{d}\tau_1 \end{aligned} \quad (27)$$

By performing a Fourier transformation to [$\mathbf{R}_u(\varepsilon)$], the power spectral density matrix of the displacement response $[\mathbf{S}_u(\omega)]$ can be obtained as follows

$$[\mathbf{S}_u(\omega)] = [\boldsymbol{\phi}][\mathbf{H}(\omega)][\boldsymbol{\phi}]^{\mathrm{T}}[\mathbf{S}_{\mathrm{P}}(\omega)][\boldsymbol{\phi}][\mathbf{H}^*(\omega)][\boldsymbol{\phi}]^{\mathrm{T}} \quad (28)$$

$$[\mathbf{H}(\omega)] = \mathbf{diag}[\mathbf{H}_j(\omega)] \quad (29)$$

$$\mathbf{H}_j(\omega) = \frac{1}{\omega_j^2 - \omega^2 + i2\zeta_j\omega_j\omega}, \quad j = 1, 2, \ldots, n \quad (30)$$

where $i = \sqrt{-1}$ is the complex number. Integrating $[\mathbf{S}_u(\omega)]$ within the frequency domain, the mean square value matrix of the structural displacement response $[\boldsymbol{\psi}_u^2]$ can be obtained as

$$[\boldsymbol{\psi}_u^2] = \int_0^\infty [\mathbf{S}_u(\omega)]\,\mathrm{d}\omega = \int_0^\infty [\boldsymbol{\phi}][\mathbf{H}(\omega)][\boldsymbol{\phi}]^{\mathrm{T}}[\mathbf{S}_{\mathrm{P}}(\omega)][\boldsymbol{\phi}][\mathbf{H}^*(\omega)][\boldsymbol{\phi}]^{\mathrm{T}}\,\mathrm{d}\omega \quad (31)$$

The mean square displacement of the kth degree of freedom becomes

$$\psi_{uk}^2 = \boldsymbol{\phi}_k \int_0^\infty [\mathbf{H}(\omega)][\boldsymbol{\phi}]^{\mathrm{T}}[\mathbf{S}_{\mathrm{P}}(\omega)][\boldsymbol{\phi}][\mathbf{H}^*(\omega)]\,\mathrm{d}\omega\boldsymbol{\phi}_k^{\mathrm{T}}, \quad k = 1, 2, \ldots, n \quad (32)$$

where $\boldsymbol{\phi}_k$ is the kth line vector of the modal matrix $[\boldsymbol{\phi}]$. From equation (32), the root mean square displacement of the kth degree of freedom can be obtained

$$\psi_{uk} = \left\{\boldsymbol{\phi}_k \int_0^\infty [\mathbf{H}(\omega)][\boldsymbol{\phi}]^{\mathrm{T}}[\mathbf{S}_{\mathrm{P}}(\omega)][\boldsymbol{\phi}][\mathbf{H}^*(\omega)]\,\mathrm{d}\omega\boldsymbol{\phi}_k^{\mathrm{T}}\right\}^{1/2}, \quad k = 1, 2, \ldots, n \quad (33)$$

Using the relationship between node displacement and element stress, the stress response of the eth element in the truss structure can be expressed as

$$\{\sigma_e(t)\} = E_e[\mathbf{B}_1]\{\boldsymbol{u}_e(t)\}, \quad e = 1, 2, \ldots, m \quad (34)$$

From equation (34), the correlation function matrix of the eth element stress response $[\mathbf{R}_{\sigma e}(\tau)]$ can be obtained by

$$[\mathbf{R}_{\sigma e}(\tau)] = E(\{\sigma_e(t)\}\{\sigma_e(t+\tau)\}^{\mathrm{T}}) = E_e[\mathbf{B}_1][\mathbf{R}_{ue}(\tau)][\mathbf{B}_1]^{\mathrm{T}}E_e \quad (35)$$

Furthermore, the power spectral density matrix of the stress response of the eth element $[\mathbf{S}_{\sigma e}(\omega)]$ can be obtained

$$[\mathbf{S}_{\sigma e}(\omega)] = E_e[\mathbf{B}_1][\mathbf{S}_{ue}(\omega)][\mathbf{B}_1]^{\mathrm{T}}E_e \quad (36)$$

Then, the mean square value matrix of the eth element stress response $[\boldsymbol{\psi}_{\sigma e}^2]$ becomes

$$[\boldsymbol{\psi}_{\sigma e}^2] = E_e[\mathbf{B}_1][\boldsymbol{\psi}_{ue}^2][\mathbf{B}_1]^{\mathrm{T}}E_e \quad (37)$$

Finally, the root mean square value matrix of the eth element stress response can be expressed as

$$[\boldsymbol{\psi}_{\sigma e}] = \{E_e[\mathbf{B}_1][\boldsymbol{\psi}_{ue}^2][\mathbf{B}_1]^{\mathrm{T}}E_e\}^{1/2} \quad (38)$$

4 NUMERICAL CHARACTERISTICS OF STOCHASTIC SMART STRUCTURAL STATIONARY RANDOM RESPONSE

4.1 Numerical characteristics analysis of dynamic characteristics by random factor method

The following parameters corresponding to ζ_j, ρ_e, A_e, l_e, E_e, ρ_e^{C}, A_e^{C}, l_e^{C}, and c_{33e} are simultaneously considered as random variables [**21**]. From equation (20), it can be easily observed that E_e^{C} is a random variable. The randomness of material and geometrical properties will result in randomness of the matrices $[\mathbf{K}]$ and $[\mathbf{M}]$, and consequently the natural frequencies ω_j and natural modal matrix $[\boldsymbol{\phi}]$.

In the following, the computing expression of the mean value and standard deviation of jth order natural frequency can be, respectively, deduced by means of the algebra synthesis method

$$\mu_{\omega_j} = \bar{\omega}_j \left\{\left[1 + \nu_Z^2 + \nu_\rho^2 + \nu_Z^2\nu_\rho^2 - c_{E\rho}\cdot\nu_E\cdot\left(\nu_Z^2 + \nu_\rho^2 + \nu_Z^2\nu_\rho^2\right)^{1/2}\right]^2 - \frac{1}{2}\left[\nu_E^2 + \nu_Z^2 + \nu_\rho^2 + \nu_Z^2\nu_\rho^2 - 2c_{E\rho}\cdot\nu_E\cdot\left(\nu_Z^2 + \nu_\rho^2 + \nu_Z^2\nu_\rho^2\right)^{1/2}\right]\right\}^{1/4} \quad (39)$$

$$\sigma_{\omega_j} = \bar{\omega}_j \left\{\left[1 + \nu_Z^2 + \nu_\rho^2 + \nu_Z^2\nu_\rho^2 - c_{E\rho}\cdot\nu_E\cdot\left(\nu_Z^2 + \nu_\rho^2 + \nu_Z^2\nu_\rho^2\right)^{1/2}\right] - \left\{\left[1 + \nu_Z^2 + \nu_\rho^2 + \nu_Z^2\nu_\rho^2 - c_{E\rho}\cdot\nu_E\cdot\left(\nu_Z^2 + \nu_\rho^2 + \nu_Z^2\nu_\rho^2\right)^{1/2}\right]^2 - \frac{1}{2}\left[\nu_E^2 + \nu_Z^2 + \nu_\rho^2 + \nu_Z^2\nu_\rho^2 - 2c_{E\rho}\cdot\nu_E\cdot\left(\nu_Z^2 + \nu_\rho^2 + \nu_Z^2\nu_\rho^2\right)^{1/2}\right]\right\}^{1/2}\right\}^{1/2}$$

$$\nu_z = \frac{\sqrt{4\nu_l^2 + 2\nu_l^4}}{1 + \nu_l^2} \quad (40)$$

where $\bar{\omega}_j$ can be obtained by the structural conventional dynamic characteristic analysis for deterministic structures. Two extreme situations exist for the values of the correlation coefficient $c_{E\rho}$. If the variables E and ρ are independent, then $c_{E\rho} = 0$. If E is completely correlative with ρ, then $c_{E\rho} = 1$. In accordance with the properties of common materials, it can be found that the elastic modulus E is usually positive correlative with the density ρ, and that the degree of correlation is rather high. Practical values for the correlative coefficient $c_{E\rho}$ are suggested in the range of 0.5–0.9 [**24–26**].

Similarly, the randomness of each element ($\boldsymbol{\phi}_{ij}$) of modal matrix is equal and can be expressed as

$$\mu_{\boldsymbol{\phi}_{ij}} = \bar{\phi}_{ij}\left[1 + \frac{1}{2}\left(\nu_\rho^2 + \nu_A^2 + \nu_l^2 + \nu_\rho^2\nu_A^2 + \nu_\rho^2\nu_l^2 + \nu_A^2\nu_l^2 + \nu_\rho^2\nu_A^2\nu_l^2\right)\right]^{1/4} \tag{41}$$

$$\sigma_{\boldsymbol{\phi}_{ij}} = \bar{\phi}_{ij}\left\{1 + \nu_\rho^2 + \nu_A^2 + \nu_l^2 + \nu_\rho^2\nu_A^2 + \nu_\rho^2\nu_l^2 + \nu_A^2\nu_l^2 + \nu_\rho^2\nu_A^2\nu_l^2 - \left[1 + \frac{1}{2}\left(\nu_\rho^2 + \nu_A^2 + \nu_l^2 + \nu_\rho^2\nu_A^2 + \nu_\rho^2\nu_l^2 + \nu_A^2\nu_l^2 + \nu_\rho^2\nu_A^2\nu_l^2\right)\right]^{1/2}\right\}^{1/2} \tag{42}$$

The deterministic values (mean values) of natural modal shape and modal matrix can be obtained by means of the conventional dynamic analysis method.

4.2 Numerical characteristics of the stationary random response

The randomness of the structural damping, natural frequencies, modeshapes, and excitations will result in randomness in the structural dynamic responses of the closed-loop control system, corresponding to the displacement and dynamic stress. In this section, expressions for the numerical characteristics corresponding to the mean value and standard deviation of the structural stationary response random variables are derived.

From equation (32), by means of the random variable's functional moment method [**25**], the mean value and standard deviation of the mean square displacement for the kth degree of freedom value can be obtained

$$\mu_{\psi_{uk}^2} = \int_0^\infty \mu_{\boldsymbol{\phi}_k}\mu_{[\mathbf{H}(\omega)]}\mu_{[\boldsymbol{\phi}]^{\mathrm{T}}}\mu_{[\mathbf{S}_{\mathrm{P}}(\omega)]}\mu_{[\boldsymbol{\phi}]}\mu_{[\mathbf{H}^*(\omega)]}\mu_{\boldsymbol{\phi}_k^{\mathrm{T}}}\,\mathrm{d}\omega \tag{43}$$

$$\begin{aligned}\sigma_{\psi_{uk}^2} = \Bigg\{\int_0^\infty \Big\{&\left\{\sigma_{\boldsymbol{\phi}_k}\mu_{[\mathbf{H}(\omega)]}\mu_{[\boldsymbol{\phi}]^{\mathrm{T}}}\mu_{[\mathbf{S}_{\mathrm{P}}(\omega)]}\mu_{[\boldsymbol{\phi}]}\mu_{[\mathbf{H}^*(\omega)]}\mu_{\boldsymbol{\phi}_k^{\mathrm{T}}}\right\}^2 \\ &+ \left\{\mu_{\boldsymbol{\phi}_k}\sigma_{[\mathbf{H}(\omega)]}\mu_{[\boldsymbol{\phi}]^{\mathrm{T}}}\mu_{[\mathbf{S}_{\mathrm{P}}(\omega)]}\mu_{[\boldsymbol{\phi}]}\mu_{[\mathbf{H}^*(\omega)]}\mu_{\boldsymbol{\phi}_k^{\mathrm{T}}}\right\}^2 \\ &+ \left\{\mu_{\boldsymbol{\phi}_k}\mu_{[\mathbf{H}(\omega)]}\sigma_{[\boldsymbol{\phi}]^{\mathrm{T}}}\mu_{[\mathbf{S}_{\mathrm{P}}(\omega)]}\mu_{[\boldsymbol{\phi}]}\mu_{[\mathbf{H}^*(\omega)]}\mu_{\boldsymbol{\phi}_k^{\mathrm{T}}}\right\}^2 \\ &+ \left\{\mu_{\boldsymbol{\phi}_k}\mu_{[\mathbf{H}(\omega)]}\mu_{[\boldsymbol{\phi}]^{\mathrm{T}}}\mu_{[\mathbf{S}_{\mathrm{P}}(\omega)]}\sigma_{[\boldsymbol{\phi}]}\mu_{[\mathbf{H}^*(\omega)]}\mu_{\boldsymbol{\phi}_k^{\mathrm{T}}}\right\}^2 \\ &+ \left\{\mu_{\boldsymbol{\phi}_k}\mu_{[\mathbf{H}(\omega)]}\mu_{[\boldsymbol{\phi}]^{\mathrm{T}}}\mu_{[\mathbf{S}_{\mathrm{P}}(\omega)]}\mu_{[\boldsymbol{\phi}]}\sigma_{[\mathbf{H}^*(\omega)]}\mu_{\boldsymbol{\phi}_k^{\mathrm{T}}}\right\}^2 \\ &+ \left\{\mu_{\boldsymbol{\phi}_k}\mu_{[\mathbf{H}(\omega)]}\mu_{[\boldsymbol{\phi}]^{\mathrm{T}}}\mu_{[\mathbf{S}_{\mathrm{P}}(\omega)]}\mu_{[\boldsymbol{\phi}]} \times\mu_{[\mathbf{H}^*(\omega)]}\sigma_{\boldsymbol{\phi}_k^{\mathrm{T}}}\right\}^2\Big\}\,\mathrm{d}\omega\Bigg\}^{1/2}, \quad k = 1, 2, \ldots, n\end{aligned} \tag{44}$$

$$\sigma_{[\mathbf{H}(\omega)]} = \mathbf{diag}\left\{\frac{\left\{\left[\left(2\mu_{\omega_j} + i\cdot 2\mu_{\xi_j}\omega\right)\cdot\sigma_{\omega_j}\right]^2 + \left[\left(i\cdot 2\mu_{\omega_j}\omega\right)\cdot\sigma_{\xi_j}\right]^2\right\}^{1/2}}{\left(\mu_{\omega_j}^2 - \omega^2 + i\cdot 2\mu_{\xi_j}\mu_{\omega_j}\omega\right)^2}\right\}, \quad j = 1, 2, \ldots, n \tag{45}$$

From equations (33), (43) to (45), by means of the algebra synthesis method [**26**], the mean value and standard deviation of the root mean square displacement for the kth degree of freedom value can be obtained

$$\mu_{\psi_{uk}} = \left[\frac{1}{2}\left(4\mu_{\psi_{uk}^2}^2 - 2\sigma_{\psi_{uk}^2}^2\right)^{1/2}\right]^{1/2} \tag{46}$$

$$\sigma_{\psi_{uk}} = \left[\mu_{\psi_{uk}^2} - \frac{1}{2}\left(4\mu_{\psi_{uk}^2}^2 - 2\sigma_{\psi_{uk}^2}^2\right)^{1/2}\right]^{1/2} \tag{47}$$

From equation (37), and by means of the algebra synthesis method, expressions for the mean value and standard deviation of the mean square stress for the eth element are obtained

$$\mu_{[\boldsymbol{\psi}_{\sigma e}^2]} = (\mu_E^2 + \sigma_E^2)[\mathbf{B}_1]\mu_{[\boldsymbol{\psi}_{ue}^2]}[\mathbf{B}_1]^{\mathrm{T}}, \quad e = 1, 2, \ldots, m \tag{48}$$

$$\begin{aligned}\sigma_{[\boldsymbol{\psi}_{\sigma e}^2]} = \Big\{&(\mu_E^2 + \sigma_E^2)^2([\mathbf{B}_1]\sigma_{[\boldsymbol{\psi}_{ue}^2]}[\mathbf{B}_1]^{\mathrm{T}})^2 \\ &+ (4\mu_E^2\sigma_E^2 + 2\sigma_E^4)([\mathbf{B}_1]\mu_{[\boldsymbol{\psi}_{ue}^2]}[\mathbf{B}_1]^{\mathrm{T}})^2 \\ &+ (4\mu_E^2\sigma_E^2 + 2\sigma_E^4)([\mathbf{B}_1]\sigma_{[\boldsymbol{\psi}_{ue}^2]}[\mathbf{B}_1]^{\mathrm{T}})^2\Big\}^{1/2}, \\ &e = 1, 2, \ldots, m\end{aligned} \tag{49}$$

From equations (38), (48), and (49), and by means of the algebra synthesis method, expressions for the numerical characteristics of the root mean square stress for the eth element are obtained as

$$\mu_{[\boldsymbol{\psi}_{\sigma e}]} = \left[\frac{1}{2}\left(4\mu_{[\boldsymbol{\psi}_{\sigma e}^2]}^2 - 2\sigma_{[\boldsymbol{\psi}_{\sigma e}^2]}^2\right)^{1/2}\right]^{1/2}, \quad e = 1, 2, \ldots, m \tag{50}$$

$$\sigma_{[\psi_{\sigma e}]} = \left[\mu_{[\psi^2_{\sigma e}]} - \frac{1}{2}\left(4\mu^2_{[\psi^2_{\sigma e}]} - 2\sigma^2_{[\psi^2_{\sigma e}]}\right)^{1/2} \right]^{1/2}, \quad e = 1, 2, \ldots, m \tag{51}$$

5 EXAMPLE

To illustrate the method, a 25-bar space smart truss structure shown in Fig. 1 is used as an example. The material properties of the active and passive bars are given in Table 1. A ground level acceleration along with the positive direction of Y-axis acts on the structure, $F(t)$ is a Gauss stationary random process and its mean value is zero. Its self-power spectral density can be expressed as [**25**]

$$S_{FF}(\omega) = \frac{1 + 4(\xi_g \omega/\omega_g)^2}{(1 - \omega^2/\omega_g^2)^2 + 4(\xi_g \omega/\omega_g)^2} S_0 \tag{52}$$

where $\omega_g = 16.5$, $\xi_g = 0.7$, $S_0 = 19.2\,\text{cm}^2/\text{s}^3$.

In order to solve the optimal problem, two steps are adopted [**21**]. In the first step, the reliability constraints of dynamic stress and displacement are neglected, and the feedback gains are kept constant. Then, each element bar is taken as an active bar in turn and the corresponding performance function value is calculated. Based on the computational results for the dissipated energy, the optimal location of the active bar can be determined. In the second step, after the optimal placement of the active bar is obtained, the reliability constraints are imposed, and the optimization of feedback gain, that is, minimization of feedback gain will be developed.

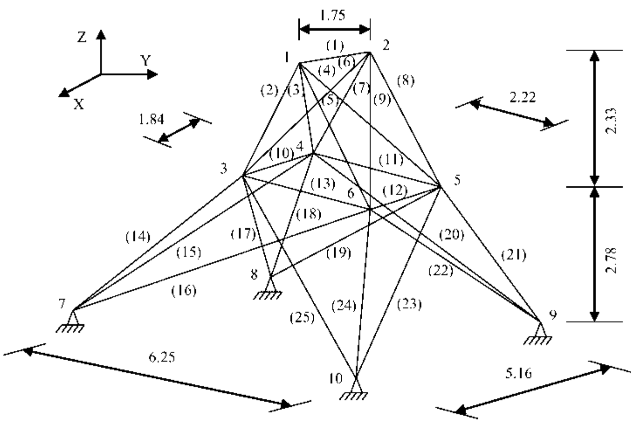

Fig. 1 Twenty-five-bar space smart truss structure (units: m)

Table 1 Physical parameters of the smart truss structure

	Active bar (PZT-4)	Passive bar (steel)
Mean value of mass density ρ (kg/m^3)	7600	7800
Mean value of elastic modulus C_{33} (N/m^2)	8.807×10^{10}	2.1×10^{11}
PZT force/electric constant e_{33} (C/m^2)	18.62	—
Dielectric constant ε_{33} (C/Vm)	5.92×10^{-9}	—
Cross-section area A (m^2)	3.0×10^{-4}	3.0×10^{-4}

5.1 Optimal placement of the active bar

For the first step, and letting the closed-loop control system feedback gains be $g = g_j = 100$, each element bar is taken as active bar in turn; the corresponding performance function value is given in Table 2.

From Table 2, it can be seen that if the 16th or 20th element is used as the active bar, the active control performance of the smart truss structure is the best. The suboptimal placement of the active bar is 15th or 12th element. The effect of active vibration control of the smart truss structure is the worst if the first element is used as the active bar.

5.2 Optimization of the feedback gain

In order to assess the control performance with the reliability constraints imposed and optimization of the feedback gain, the control results using the optimal and suboptimal placements, that is, 16th and 15th element as the active bar, respectively, are compared. The structural parameters (material properties, geometric dimensions, structural damping) and the limit values of the maximum root mean square stress and displacement are all taken to be random variables, where $\mu_{\psi^*_\sigma} = 53\,\text{MPa}$, $\mu_{\psi^*_u} = 2\,\text{mm}$ and $R^*_{\psi_\sigma} = R^*_{\psi_u} = 0.95$. Values from both deterministic and random models were obtained. In the DM, the mean values of the random variables are unity, and their standard deviations are zero. The optimal results for the feedback gains and the root mean displacement and stress responses are given in Table 3. Results for two random models are presented, in which the variation coefficients of all random variables is equal to 0.05 in the first random model (first RM), and 0.1 in the second random model (second RM). In addition, in order to verify the method, stationary random responses obtained using the Monte Carlo simulation (MCS) method are also presented in Table 3.

From Table 3, it can be seen easily that the optimal results of the feedback gains obtained by the method proposed in this paper is in excellent agreement with that of the random structural stationary random responses analysed by the MCS method, by which the validity of the method is verified. The

Table 2 Computational results of the performance function ($g = 100$)

Element (node–node)	1(1–2)	2(1–3)	3(1–4)	4(1–5)	5(1–6)	6(2–3)	7(2–4)
Value of J	96.86	118.70	115.67	135.58	132.12	137.33	129.88
Element (node–node)	8(2–5)	9(2–6)	10(3–4)	11(4–5)	12(5–6)	13(6–3)	14(7–3)
Value of J	126.55	122.31	141.26	147.54	141.26	147.54	169.97
Element (node–node)	15(7–4)	16(7–6)	17(8–3)	18(8–4)	19(8–5)	20(9–4)	21(9–5)
Value of J	189.31	196.28	176.49	163.22	182.65	196.28	169.97
Element (node–node)	22(9–6)	23(10–5)	24(10–6)	25(10–3)			
Value of J	189.31	176.49	163.22	182.65			

Table 3 Computational results of the feedback gains

	Sixteenth element used as the active bar				Fifteenth element used as the active bar			
Design variables	Original value	DM	First RM	Second RM	Original value	DM	First RM	Second RM
G	50	89.291	117.57	136.92	50	90.867	119.646	139.338
$^*G$			*117.59	*136.94			*119.650	*119.243
$\mu_{\max(\psi_{\sigma e})}$	61.196	52.992	46.307	42.457	62.297	52.993	46.308	42.459
$^*\mu_{\max(\psi_{\sigma e})}$			*46.316	*42.469			*46.312	*42.465
$\mu_{\max(\psi_{uk})}$	2.3172	1.9997	1.7466	1.5801	2.3589	1.9999	1.7468	1.5803
$^*\mu_{\max(\psi_{uk})}$			*1.7467	*1.5803			*1.7470	*1.5809
R_{ψ_σ}		0.50	0.95	0.95		0.50	0.95	0.95
R_{ψ_u}		0.52	0.97	0.97		0.52	0.97	0.97

*Dynamic analysis by the MCS method.

results show that the areas of the truss structure where the most energy is stored are the optimal location of an active bar in order to maximize its damping effect.

6 CONCLUSION

The effectiveness of using the active element and the value of feedback gains is strongly dependent on the active bar's location in the smart truss structure. The randomness of the structural parameters affects the optimal results of feedback gains obviously, the optimal value of feedback gains will increase remarkably along with the increase of the variation coefficients of these random variables. The optimal results of DM and random models are different. The optimal results of DM fulfil the normal constraints, but the results can not fulfil the reliability constrains.

REFERENCES

1 **Hurlebaus, S.** and **Gaul, L.** Smart structure dynamics. *Mech. Syst. Signal Process.*, 2006, **20**(1), 255–281.
2 **Chopra, I.** Status of application of smart structures technology to rotorcraft systems. *J. Am. Helicopter Soc.*, 2000, **45**(4), 228–252.
3 **Diwekar, A. M.** and **Yedavalli, R. K.** Smart structure control in matrix second-order form. *Smart Mater. Struct.*, 1996, **5**(4), 429–436.
4 **Wang, Q.** and **Wang, C. M.** Controllability index for optimal design of piezoelectric actuators in vibration control of beam structures. *J. Sound Vibr.*, 2001, **242**(3), 507–518.
5 **Suk, J., Boo, S.,** and **Kim, Y.** Lyapunov control law for slew maneuver using time finite element analysis. *J. Guid. Control Dyn.*, 2001, **24**(1), 87–94.
6 **Quek, S. T., Wang, S. Y.,** and **Ang, K. K.** Vibration control of composite plates via optimal placement of piezoelectric patches. *J. Intell. Mater. Syst. Struct.*, 2003, **14**(4–5), 229–245.
7 **Chen, C. C.** and **Lin, C. C.** An impedance approach for determining optimal locations and shapes of multiple induced strain actuators. *Smart Mater. Struct.*, 2005, **14**(6), 1120–1126.
8 **Peng, F. J., Ng, A.,** and **Hu, Y. R.** Actuator placement optimization and adaptive vibration control of plate smart structures. *J. Intell. Mater. Syst. Struct.*, 2005, **16**(3), 263–271.
9 **Papadrakakis, M.** and **Kotsopulos, A.** Parallel solution methods for stochastic finite element analysis using Monte Carlo simulation. *Comput. Methods Appl. Mech. Eng.*, 1999, **168**(1–4), 305–320.
10 **Hurtado, J. E.** and **Barbat, A. H.** Monte Carlo techniques in computational stochastic mechanics. *Arch. Comput. Methods Eng.*, 1998, **5**(1), 3–29.
11 **Singh, B. N., Yadav, D.,** and **Iyengar, N. G. R.** Natural frequencies of composite plates with random material properties using higher-order shear deformation theory. *Int. J. Mech. Sci.*, 2001, **43**(10), 2193–2214.
12 **Sachdeva, S. K., Nair, P. B.,** and **Keane, A. J.** Comparative study of projection schemes for stochastic finite element analysis. *Comput. Methods Appl. Mech. Eng.*, 2006, **195**(19–22), 2371–2392.

13 **Ghanem, R. G.** and **Spanos, P. D.** Spectral stochastic finite-element formulation for reliability-analysis. *J. Eng. Mech. ASCE*, 1991, **117**(10), 2351–2372.

14 **Elishakoff, I., Ren, Y. J.,** and **Shinozuka, M.** New formulation of FEM for deterministic and stochastic beams through generalization of Fuchs' approach. *Comput. Methods Appl. Mech. Eng.*, 1997, **144**(3–4), 235–243.

15 **Graham, L. L.** and **Deodatis, G.** Response and eigenvalue analysis of stochastic finite element systems with multiple correlated material and geometric properties. *Probab. Eng. Mech.*, 2001, **16**(1), 11–29.

16 **Zhao, L.** and **Chen, Q.** Neumann dynamic stochastic finite element method of vibration for structures with stochastic parameters to random excitation. *Comput. Struct.*, 2000, **77**(6), 651–657.

17 **Li, J.** and **Liao, S. T.** Dynamic response of linear stochastic structures under random excitation. *Acta Mech. Sin.*, 2002, **34**(3), 416–424.

18 **Ma, X. P., Leng, X. L., Meng, G.,** and **Fang, T.** Evolutionary earthquake response of uncertain structure with bounded random parameter. *Probab. Eng. Mech.*, 2004, **19**(3), 239–246.

19 **Li, J.** and **Chen, J. B.** Dynamic response and reliability analysis of structures with uncertain parameters. *Int. J. Numer. Methods Eng.*, 2005, **62**(2), 289–315.

20 **Bathe, K. J.** *Finite element procedures in engineering analysis*, 1995 (Prentice-Hall, Inc., New Jersey).

21 **Gao, W., Chen, J. J., Ma, H. B.,** and **Ma, X. S.** Optimal placement of active bars in active vibration control for piezoelectric intelligent truss structures with random parameters. *Comput. Struct.*, 2003, **81**(1), 53–60.

22 **Abdullah, M. M.** Optimal location and gains of feedback controllers at discrete locations, *AIAA J.*, 1998, **36**(11), 2109–2116.

23 **Chen, J. J.** and **Duan, B. Y.** Structural optimization by displaying the reliability constraints. *Comput. Struct.*, 1994, **50**(6), 777–783.

24 **Gao, W., Chen, J. J., Zhou, Y. B.,** and **Cui, M. T.** Dynamic response analysis of closed loop control system for random intelligent truss structure under random forces. *Mech. Syst. Signal Process.*, 2004, **18**(4), 947–957.

25 **Gao, W., Chen, J. J., Cui, M. T.,** and **Cheng, Y.** Dynamic response analysis of linear stochastic truss structures under stationary random excitation. *J. Sound Vibr.*, 2005, **281**(1–2), 311–321.

26 **Gao, W., Chen, J. J., Ma, J.,** and **Liang, Z. T.** Dynamic response analysis of stochastic frame structures under non-stationary random excitation. *AIAA J.*, 2004, **42**(9), 1818–1822.

APPENDIX

Notation

A	bar's cross-sectional area
A_e	eth passive bar's mass cross-sectional area
A_e^{C}	eth active bars' cross-sectional area
$[\mathbf{B}]$	input matrix
$[\mathbf{B}_1]$	element's strain matrix
$c_{E\rho}$	correlation coefficient of variables Young's modulus and mass density
c_{33e}	eth active bar's Young's modulus
$[\mathbf{C}]$	damping matrix
$\mathbf{diag}(\cdot)$	diagonal matrix with diagonal elements given in brackets
e_{33e}	eth active bar's PZT force/electrical constant
E	Young's modulus
E_e	eth passive bar's Young's modulus
$\{\boldsymbol{F}(t)\}$	stationary random excitation
$\{\boldsymbol{F}_{\mathrm{C}}(t)\}$	control force vector
$[\mathbf{G}]$	gain matrix
$[\mathbf{h}(t)]$	impulse response function matrix
$[\mathbf{H}(\omega)]$	frequency response function matrix
$[\mathbf{H}^*(\omega)]$	conjugate matrix of $[\mathbf{H}(\omega)]$
$[\mathbf{K}^{(e)}]$, $[\mathbf{M}^{(e)}]$	eth element's stiffness and mass matrices, respectively
$[\mathbf{K}]$, $[\mathbf{M}]$	global stiffness and mass matrices, respectively
l_e	eth passive bar's length
l_e^{C}	eth active bars' length
L	bar's length
m	number of the structural elements
$\max(\cdot)$	maximum value of the variables given in brackets
n	number of the natural frequencies
$\{\boldsymbol{P}(t)\}$	stationary random excitation vector
$R^*_{\psi_u}$	given value of reliability of the maximum root mean square displacement responses
$R^*_{\psi_\sigma}$	given value of reliability of the maximum root mean square stress responses
$[\mathbf{R}_{\mathrm{P}}(\tau - \tau_1 + \varepsilon)]$	correlation function matrix of $\{\boldsymbol{P}(t)\}$
$[\mathbf{R}_u(\varepsilon)]$	correlation function matrix of structural displacement response
$[\mathbf{R}_{\sigma e}(\tau)]$	correlation function matrix of the eth element's stress response
$[\mathbf{S}_{\mathrm{P}}(\omega)]$	equivalent one-side power spectral density matrix of $\{\boldsymbol{P}(t)\}$
$[\mathbf{S}_u(\omega)]$	power spectral density matrix of displacement response
$[\mathbf{S}_{\sigma e}(\omega)]$	power spectral density matrix of the stress response of the eth element
$\{\boldsymbol{u}(t)\}$, $\{\dot{\boldsymbol{u}}(t)\}$, $\{\ddot{\boldsymbol{u}}(t)\}$	displacement, velocity and acceleration vectors, respectively

$\{\boldsymbol{u}_e(t)\}$	displacement response of the nodal point of the eth element
$\boldsymbol{Y}(t)$	output vector
ε_{33e}	the eth active bar's dielectric constant
μ	mean value of random variable
ν	variation coefficient of random variable
ξ_j	jth order mode damping of structure
ρ	mass density
ρ_e	eth passive bar's mass density
ρ_e^{C}	eth active bars' mass density
σ	mean variance of random variable
$\{\sigma_e(t)\}$	stress response of the eth element
$[\boldsymbol{\phi}]$	normal modal matrix
$\left[\boldsymbol{\psi}_u^2\right]$	mean square value matrix of structural displacement response
ψ_{uk}^2	mean square value of the kth degree of freedom of dynamic displacement response
ψ_{uk}	root mean square value of the kth degree of freedom of dynamic displacement response
ψ_u^*	given limit values of the maximum root mean square displacement responses
$\left[\boldsymbol{\psi}_{\sigma e}^2\right]$	mean square value matrix of the eth element stress response
$\psi_{\sigma e}$	root mean square value of structural dynamic stress response
ψ_σ^*	given limit values of the maximum root mean square stress responses
ω_j	jth order natural frequency